Journal of Industrial and Engineering Chemistry 18 (2012) 312–316

Contents lists available at SciVerse ScienceDirect

Journal of Industrial and Engineering Chemistry

journal homepage: www.elsevier.com/locate/jiec

Study on the wet processable antimony tin oxide (ATO) transparent electrode for PLEDs

In Sung Song [a], Soo Won Heo [a], Jun Hee Lee [b], Jung Rim Haw [a], Doo Kyung Moon [a,*]

[a] Department of Materials Chemistry and Engineering, Konkuk University, 1 Hwayang-dong, Gwangjin-gu, Seoul 143-701, Republic of Korea
[b] Department of Advanced Materials Engineering, Dong-A University, Saha-gu, Busan 604-714, Republic of Korea

ARTICLE INFO

Article history:
Received 2 March 2011
Accepted 5 April 2011
Available online 7 November 2011

Keywords:
Polymer light emitting diodes (PLEDs)
Indium tin oxide (ITO)
Antimony tin oxide (ATO)
Spin coating

ABSTRACT

A polymer light emitting diodes (PLEDs) was fabricated using the wet processable antimony tin oxide (ATO) as the transparent electrode by spin coating method. PLED were fabricated with ATO (or ITO)/PEDOT:PSS/polymer/BaF_2/Ba/Al configurations. Electrical and optical properties of ATO transparent electrode were measured. Transmittance of ATO thin film was more than 90% in the visible region, sheet resistance was 30 $\Omega/\square$ and had a strong solvent resistance. The maximum brightness and maximum efficiency of PLED device using an ATO transparent electrode was 3637 cd/m^2 and 1.03 cd/A, respectively.

1. Introduction

Transparent conducting oxide (TCO) film is the thin film which has more than 80% of transmittance in visible region (380–780 nm) and a specific resistance of 10^{-3} Ω cm or less for electronic devices [1–9]. TCO film has been widely used as the transparent electrode of various flat panel displays (FPDs) such as antistatic film, thermal reflective film, organic photovoltaic cells (OPVs) [10–15], organic thin film transistors (OTFTs), liquid crystal display (LCD) and organic light emitting diodes (OLEDs) [16–19]. Therefore, a variety of materials such as cadmium, tin, indium and zinc have been studied. The transparent electrodes to which these materials are applied include fluorine-doped tin oxide (FTO), cadmium stannate (CTO) and indium tin oxide (ITO). Among them, the ITO thin film in which tin is doped to In_2O_3 has been commonly used as a transparent electrode material owing to low resistance and high transparency [20,21]. A lot of methods are used to product this thin film including a sputtering method [22,23], chemical vapor deposition (CVD), thermal evaporation, e-beam evaporation [24], reactive ion plating, spray pyrolysis [25] and chemical solution growth. With an enormous growth of opto-electronic device market, however, a demand for ITO has significantly increased due to limited indium deposits, its price has skyrocketed every year. In addition, it has disadvantages of inability to apply roll-to-roll process and high equipment and processing unit price when ITO thin film is formed through vacuum deposition process such as magnetron sputtering.

In this study, we use antimony which has low price and is available to wet process instead of indium to fabricate low price transparent electrode [26,27]. Furthermore, as ATO has −5.1 eV of work function, it is expected that ATO would improve luminous efficiency due to superior hole injection greater than ITO (4.7 eV) by 0.4 eV. Then, the morphology of the fabricated ATO thin film was observed, and measured transmittance according to thickness, solvent resistance of thin film and sheet resistance ($\Omega/\square$) by annealing temperature. Finally, PLED devices were fabricated and characterized *I–V–L* properties.

2. Materials and measurements

2.1. Materials

Orange color polymer was used for the emitting layer. The antimony tin oxide solution was purchased from Keeling & Walker and poly (3,4-ethylenedioxy thiophene) blended with poly (styrenesulfonate) (PEDOT:PSS, AI4083) was purchased from Baytron, respectively.

2.2. Measurements

All thin films were fabricated using a GMC2 spin coater (Gensys, Korea), and their thickness was measured using an alpha step 500 surface profiler (KLA-Tencor). The absorbance and transmittance of the ATO film was measured using an Agilent 8453 UV-visible

---

* Corresponding author. Tel.: +82 2 450 3498; fax: +82 2 444 0765.
E-mail address: dkmoon@konkuk.ac.kr (D.K. Moon).

1226-086X/$ – see front matter © 2011 The Korean Society of Industrial and Engineering Chemistry. Published by Elsevier B.V. All rights reserved.
doi:10.1016/j.jiec.2011.11.051

spectrometer (HP Agilent), and the conductivity was measured with a 4-point probe station (MST6000C). Also, the electro-optical properties of the fabricated device were characterized using a Keithley 2400 source meter unit (Keithley) and a PR 670 spectra scan (Photo Research), while the surface morphology of thin film was measured using an atomic force microscope (AFM, PSIA XE-150) and transmission electron microscope (TEM, JEOL JEM-2010).

3. Experiments

3.1. ITO cleaning and solvent resistance test of antimony tin oxide thin film

To fabricate PLED which has used ATO as transparent electrode, a solvent resistance test has been conducted on the ATO thin film. To clean the ITO glass (10 $\Omega/\square$, Samsung Corning), sonication was performed using detergent (Alconox® in deionized water, 10%), acetone, IPA (isopropylalcohol), and deionized water, in the order listed, for 20 min respectively. Moisture was blown thoroughly with N_2 gas. In order to ensure the complete removal of all remaining water, the ITO was baked on a hot plate for 10 min at 120 °C. To administer hydrophilic treatment to the glass surface, it was cleaned for 10 min in a UVO cleaner.

To measure solvent resistance, the ATO solution which has been filtered with 5 μm PTFE syringe filter on the cleaned ITO glass was coated at 1000 rpm. Then, it was annealed at 300 °C for 3 h to remove residual solvent. As a result, 350 nm thin film was obtained. The fabricated ATO thin film was rinsed with DI water, chlorobenzene, and chloroform.

3.2. Transmittance test by change in thickness

To observe transmittance and change in thickness by the number of spin coating, spin-coasting speed has been set to 1000 rpm, and coating was repeated six times. In case of a repetitive coating sample, coating was done once. After baking the film on the hot plate (110 °C) for ten 10 min and cooling it down at room temperature, it was coated again. The thickness has been measured using an alpha step 500 surface profiler. In addition, the transmittance by ATO thickness has been measured by the UV–visible spectroscopy.

3.3. Sheet resistance test by thickness and annealing temperature

Sheet resistance by ATO thickness and annealing temperature has been measured. With 350 nm and 720 nm of thickness, a sample has been fabricated by raising annealing temperature from 100 °C to 600 °C by 100 °C. After 5-h annealing, sheet resistance was measured using 4-point probe station (Mc Science, Korea).

3.4. Fabrication of PLEDs

The ATO thin film on the glass has been patterned, and ITO was cleaned after patterning with photolithography method. PEDOT:PSS was blended for 24 h after being filtered with a 0.45 μm PTFE syringe filter. Orange light emitting polymer was dissolved in chlorobenzene (0.5 wt%) and blended for 24 h. After filtering it with a 5 μm PTFE syringe filter, it was spin-coated on ATO thin film with the condition stated in Table 1. The structure of fabricated PLED is shown in Fig. 1. After baking PEDOT:PSS at 110 °C for 20 min and light emitting polymer at 90 °C for an hour, residual solvents were removed. To deposit electron injection layer and electrode materials, they were transferred to the high vacuum chamber (1×10^{-6} torr or less) of thermal evaporator. All devices were deposited in order of BaF_2 (0.1Å/s, 2 nm), Ba (0.2Å/s, 2 nm) and Al (5Å/s, 200 nm). To protect the organic and electrode layers from moisture and oxygen, they were encapsulated in a glove box with cover glass. The completed devices were electrically and optically characterized using Keithley 2400 source meter unit and PR 670. In addition, the morphology of the fabricated thin film was observed through atomic force microscope.

Table 1
Fabrication structure and thickness of devices.

Devices	Fabrication structure and thickness
Device I	ATO (350 nm)
Device II	ATO (720 nm)
Reference	ITO (170 nm)

I, II and Ref/PEDOT:PSS (25 nm)/orange polymer (80 nm)/BaF_2 (2 nm)/Ba (2 nm)/Al (200 nm).

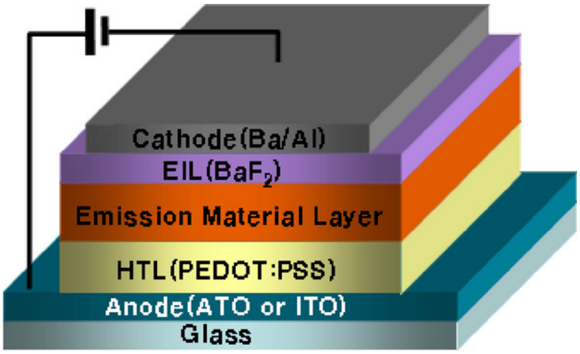

Fig. 1. Structure of PLED in this study.

4. Results and discussion

4.1. Characteristics of TEM image and solvent resistance

The TEM image of ATO thin film was provided from P&H Tech (Korea) have been observed. According to the TEM images in Fig. 2, it is confirmed that a network was formed by ATO. Through the network, a hole moves, and conductivity reveals. It is also available as anode. Furthermore, because the part in which a network is not formed yet is still empty, the optical transmittance of ATO film is superior.

Almost no difference was detected in absorbance before and after rinsing ATO thin film with DI water or an organic solvent such

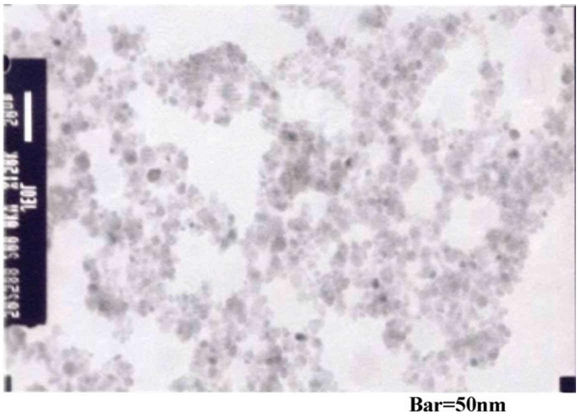

Fig. 2. Transmission electron microscopy (TEM) image of ATO thin film.

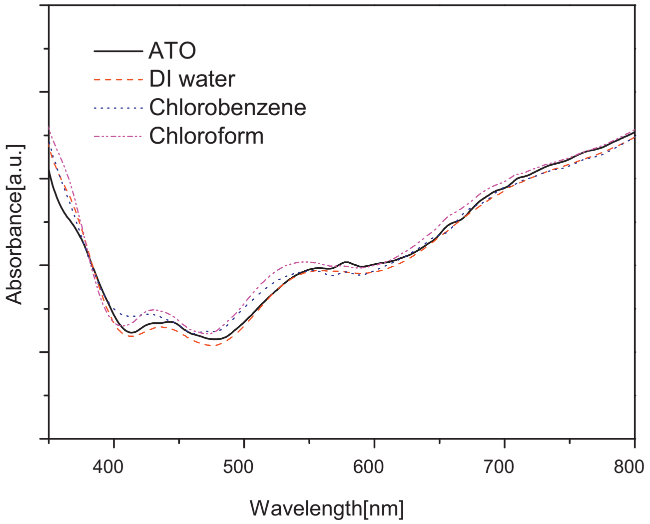

Fig. 3. Absorption spectrum of ATO thin film, rinsing with various solvents.

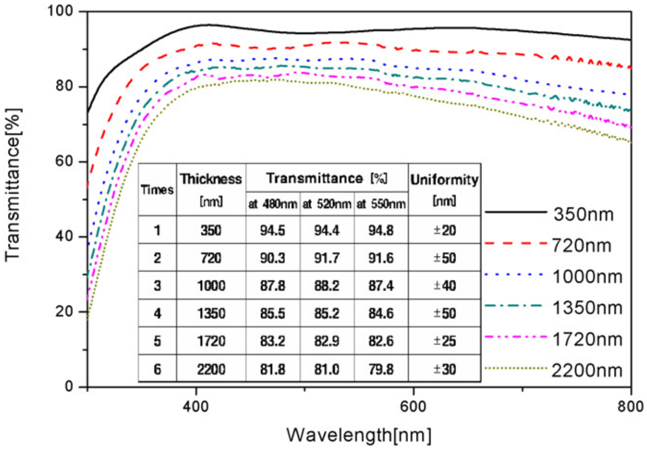

Times	Thickness [nm]	Transmittance [%]			Uniformity [nm]
		at 480nm	at 520nm	at 550nm	
1	350	94.5	94.4	94.8	±20
2	720	90.3	91.7	91.6	±50
3	1000	87.8	88.2	87.4	±40
4	1350	85.5	85.2	84.6	±50
5	1720	83.2	82.9	82.6	±25
6	2200	81.8	81.0	79.8	±30

Fig. 4. Transmittance of ATO by thickness.

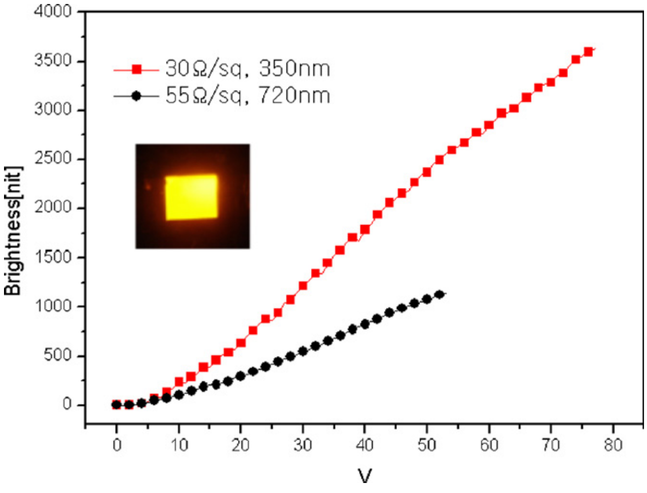

Fig. 5. Brightness–voltage graph of devices. Inset, device emitting image.

as chlorobenzene and chloroform (Fig. 3). In other words, ATO thin film was strong solvent-resistant against DI water and organic solvent, which means that when ATO was used as a transparent electrode, even though water-based PEDOT:PSS and polymer solution dissolved organic solvent are coated, no interaction occurs in the interface with the ATO layer. Hence, if the ATO thin film is applied as the transparent electrode of PLED, even though a layer is formed with wet process using water or organic solvent-based solution on the ATO film, charge injection is not impeded.

4.2. Transmittance measurement by change in thickness

After setting ATO spin speed to 1000 rpm, spin coating was conducted repeatedly from 1 to 6 times. Then, the thickness and transmittance of each thin film were measured, and the results are shown in Fig. 4. In particular, transmittance recorded 94.8% and 91.6% (at wavelength 550 nm) respectively when the ATO thin film has 350 nm and 720 nm-thick. Then, more than 90% of transmittance was detected in the visible region, which was greater than ITO in which 87% of transmittance was observed at wavelength 550 nm. In case of 1000 nm thick, in addition, transmittance was almost the same with ITO with 87.4%. When transmittance was only considered, therefore, ATO could be substituted with ITO provided that it is 1000 nm or less in terms of thickness.

4.3. Characterization of sheet resistance by thickness and annealing temperature

Table 2 shows the result of the characteristics of sheet resistance by annealing temperature when the ATO thin film was 350 nm and 720 nm-thick. In case the film was 1000 nm or thicker, optical transmittance decreased. In addition, poor characteristics were detected at fabrication of PLED due to high sheet resistance. The sheet resistance decreased as annealing temperature increased. At 500°C, it started to increase again. It appears that this phenomenon occurs because of interruption in carrier motion after ATO was thermally degraded at 500 °C or higher temperatures.

4.4. Characterization of PLEDs

Figs. 5 and 6 show brightness–voltage and efficient–brightness graphs respectively. In case of Device I (30 Ω/□ of sheet resistance), maximum brightness and maximum efficiency recorded 3637 cd/m^2 and 1.03 cd/A respectively, which were greater than the maximum brightness (1210 cd/m2) and maximum efficiency (0.37 cd/A) of Device II (50 Ω/□ of sheet resistance) by 3 and 2.7 times respectively. Because Device I is smaller than Device II in terms of the sheet resistance of ATO transparent electrode, hole injection becomes easy, and recombination of hole and electron can take place more easily on the

Table 2
Sheet resistance of various annealing temperature and thickness.

Temperature	100 °C	200 °C	300 °C	400 °C	500 °C	600 °C	Thickness
Sheet resistance [Ω/□]	130 K	15 K	2 K	250	30	75	350 nm
	180 K	13 K	5 K	612	55	102	720 nm

Table 3
Characteristics of devices.

Structures	Turn on voltage [V]	Max brightness [cd/m^2]	Max efficiency [cd/A]	CIE coordinates	λ_{max} [nm]	Full width at half maximum [FWHM, nm]
Device I (30 Ω/□, 350 nm)	2.5	3637	1.03	(0.57, 0.42)	584	120
Device II (55 Ω/□, 720 nm)	2.5	1210	0.37	(0.57, 0.42)	586	130
Reference (15 Ω/□, 170 nm)	1.5	19,585	1.30	(0.57, 0.42)	586	118

I, II and Ref/PEDOT:PSS (25 nm)/orange polymer (80 nm)/BaF$_2$ (2 nm)/Ba (2 nm)/Al (200 nm).

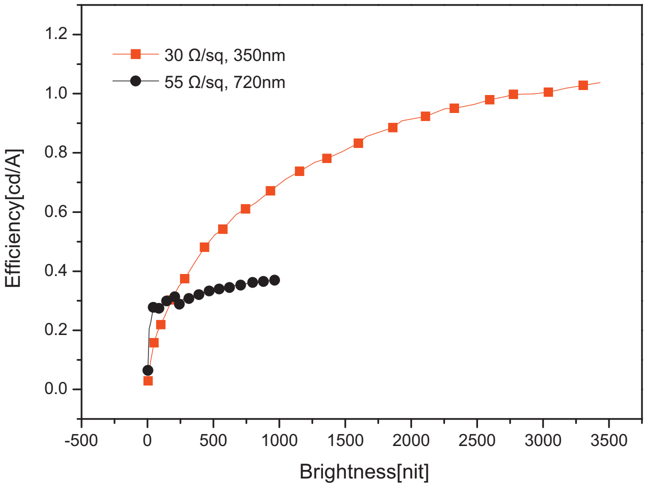

Fig. 6. Efficiency–brightness graph of devices.

emitting layer. That is why maximum brightness and maximum efficiency were high in Device I. The pictures in Fig. 5 show the emitting light of Device I. In Table 3, Device I, Device II and ITO were compared when they were used as transparent electrode. Device I was the best among the devices in which ATO was used as anode. In terms of turn-on voltage, Device I was greater than the device in which ITO was used as anode by 1.0 V. In terms of maximum brightness, Device I was very low with 18%, compared to the device in which ITO was used. In terms of maximum efficiency, Device I (ATO was used) was the same with the device in which ITO was used. In terms of CIE coordinates, in addition, ATO and ITO had same coordinates. Therefore, it has been proven that ATO can be substituted with ITO anytime through improvement. Fig. 7 demonstrates the EL spectrum of ITO, Device I and Device II. While Device II recorded 130 nm in terms of Full Width at Half Maximum (FWHM), Device I showed better color purity with 120 nm, which was almost same with ITO (118 nm). Therefore, it has been confirmed that ATO transparent electrode was not greater than ITO transparent electrode in terms of absorption or diffusion of emitting light.

Besides the said two devices, devices have been fabricated using an ATO transparent electrode which has various sheet resistances. However, whole emission did not occur, or emission characteristics were very low. Therefore, it has been confirmed that device characteristics can greatly vary by the sheet resistance and transparency of ATO thin film. In other words, the sheet resistance of ATO thin film was dependent on thickness and annealing temperature.

As shown in an energy band diagram in Fig. 8, ATO was greater than ITO in terms of work function. Because of easy hole injection to the PEDOT:PSS layer, in other words, it was expected that characteristics would increase. However, maximum brightness and maximum efficiency were low with 18% and 100% of ITO. In other words, the emitting characteristics are determined by various factors (ex: sheet resistance, transparency, interface between layers, etc.) as well as energy band gap. According to an observation on the surface of ATO and ITO using AFM images (Fig. 9), ATO thin film (6.63 nm) was greater than ITO (5.40 nm) in terms of roughness. In fact, it has been confirmed that carrier injection to the PEDOT-PSS layer was not easier in ATO than in ITO.

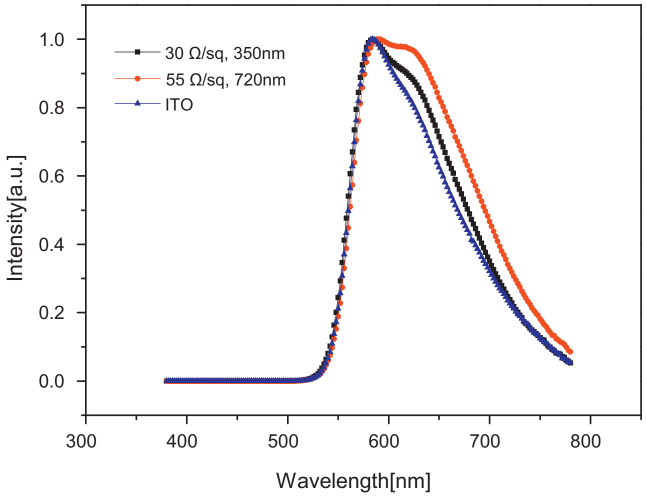

Fig. 7. EL spectrum of devices.

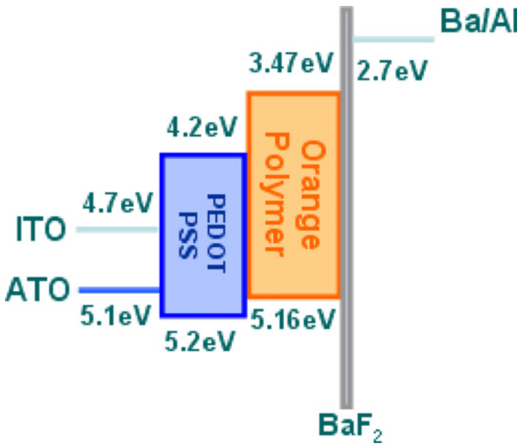

Fig. 8. Energy band diagram of devices.

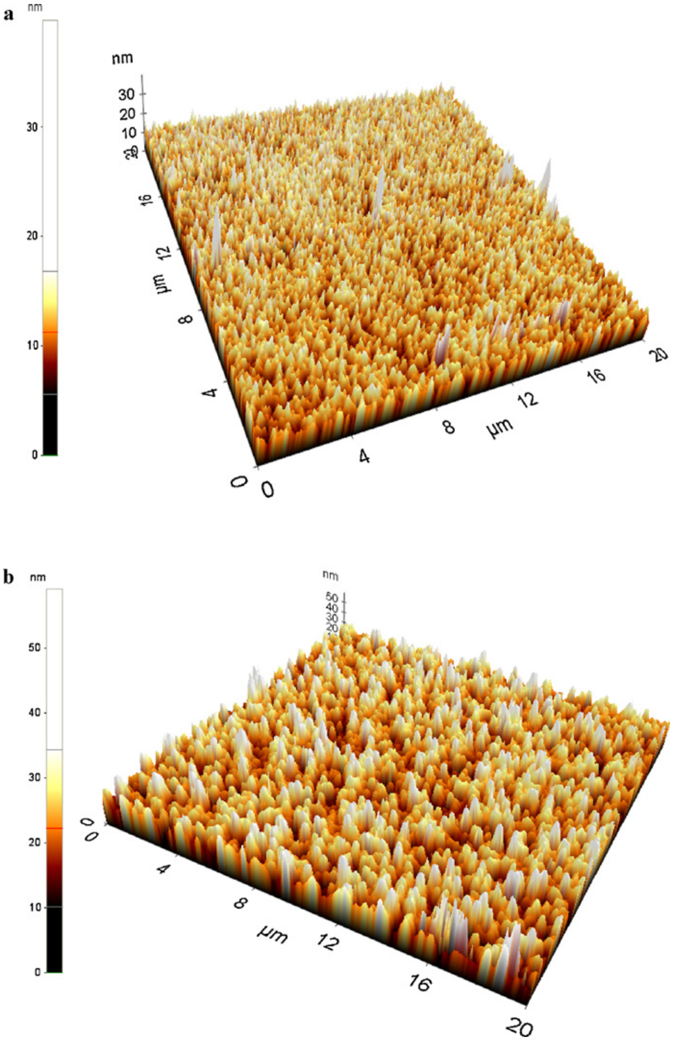

Fig. 9. AFM images of ITO and ATO. (a) Surface morphology of ITO (RMS: 5.40 nm) and (b) surface morphology of ATO (RMS: 6.63 nm).

That is why an ATO-based device has been lower than an ITO-based device in terms of electrical characteristics.

5. Conclusion

This paper was studied the characteristics of thin film and device structure optimization using antimony tin oxide (ATO) which can be substituted with ITO transparent electrode and makes wet process possible. To use ATO as transparent electrode, a solvent resistance test was performed using DI water and an organic solvent such as chlorobenzene and chloroform. As a result, strong solvent resistance was observed in all solvents. In addition, it has been confirmed that a channel through which a carrier can move on the thin film surface of the ATO transparent electrode which was observed through TEM was well formed. According to the test, the sample in which a 350 nm-thick film was annealed at 500 °C for 5 h showed the lowest sheet resistance (30 Ω/□) with the highest transparency. The ATO/PEDOT:PSS-structured device which has been fabricated through this sample was 3637 cd/cm^2 and 1.03 cd/A in terms of maximum brightness and maximum efficiency. In addition, a possibility that a wet processable ATO transparent electrode could be substituted with ITO was observed.

Acknowledgments

This work was supported by the Energy Efficiency & Resources (2008K00203) of the Korea Institute of Energy Technology Evaluation and Planning (KETEP) grant funded by the Korea government Ministry of Knowledge Economy and by Business for Cooperative R&D between Industry, Academy, and Research Institute funded Korea Small and Medium Business Administration (00035745-1) in 2009.

References

[1] H.N. Wanka, M.B. Schubert, E. Lotter, Sol. Energy Mater. Sol. Cells 41 (1996) 519.
[2] K. Imamori, A. Masuda, H. Matsumura, Thin Solids Films 395 (2001) 147.
[3] H. Hosono, H. Ohta, M. Orita, K. Ueda, M. Hirano, Vacuum 66 (2002) 419.
[4] L. Wang, J.S. Swensen, E. Polikarpov, D.W. Matson, C.C. Bonham, W. Bennett, D.J. Gaspar, A.B. Padmaperuma, Org. Electron. 11 (2010) 1555.
[5] Y.F. Lan, W.C. Peng, Y.H. Lo, J.L. He, Org. Electron. 11 (2010) 670.
[6] X. Xianwu, P. Zhiyong, D. Ying, Y. Lina, H. Shenghao, Appl. Surf. Sci. 253 (2007) 3345.
[7] T. Minami, Thin Solid Films 516 (2008) 1314.
[8] A. Subrahmanyam, U.K. Barik, J. Phys. Chem. Solids 66 (2005) 817.
[9] G.J. Exarhos, X.D. Zhou, Thin Solid Films 515 (2007) 7025.
[10] J.Y. Lee, M.H. Choi, S.W. Heo, D.K. Moon, Synth. Met. 161 (2011) 1.
[11] J.Y. Lee, M.H. Choi, H.J. Song, D.K. Moon, J. Polym. Sci. A: Polym. Chem. 48 (2010) 4875.
[12] J.Y. Lee, Y.J. Kwon, J.W. Woo, D.K. Moon, J. Ind. Eng. Chem. 14 (2008) 810.
[13] K.W. Song, J.Y. Lee, S.W. Heo, D.K. Moon, J. Nanosci. Nanotechnol. 10 (2010) 99.
[14] J.Y. Lee, S.W. Heo, H. Choi, Y.J. Kwon, J.R. Haw, D.K. Moon, Sol. Energy Mater. Sol. Cells 93 (2009) 1932.
[15] J.Y. Lee, W.S. Shin, J.R. Haw, D.K. Moon, J. Mater. Chem. 19 (2009) 4938.
[16] I.S. Song, S.W. Heo, J.Y. Lee, D.K. Moon, J. Ind. Eng. Chem. 17 (2011) 651.
[17] J. Chung, K.H. Kim, J.C. Lee, M.K. Kim, H.J. Shin, Org. Electron. 9 (2008) 869.
[18] H.J. Song, J.Y. Lee, I.S. Song, D.K. Moon, J.R. Haw, J. Ind. Eng. Chem. 17 (2011) 352.
[19] S. Woo, J. Kim, G. Cho, K. Kim, H. Lyu, Y. Kim, J. Ind. Eng. Chem. 15 (2009) 716.
[20] J. Szczyrbowski, K. Schmalzbauer, H. Hoffmann, Thin Solid Films 137 (1986) 169.
[21] K.L. Chopra, S. Major, D.K. Pandya, Thin Solid Films 102 (1983) 1.
[22] T. Karasawa, Y. Miyata, Thin Solid Films 223 (1993) 135.
[23] W.K. Lee, T. Machino, T. Sugihara, Thin Solid Films 224 (1993) 105.
[24] H.J. Krokoszinski, R. Oesterlein, Thin Solid Films 187 (1990) 179.
[25] L.A. Ryabova, V.S. Salun, L.A. Serbinov, Thin Solid Films 92 (1982) 327.
[26] K. Ravichandran, P. Philominathan, Mater. Lett. 62 (2008) 2980.
[27] M.R.S. Castro, P.W. Oliveira, H.K. Schmidt, Semicond. Sci. Technol. 23 (2008) 035013.